



LAWRENCE
LIVERMORE
NATIONAL
LABORATORY

Increasing robustness of indirect drive capsule designs against short wavelength hydrodynamic instabilities

S. W. Haan, M. C. Herrmann, T. R. Dittrich, A. J. Fetterman, M. M. Marinak, D. H. Munro, S. M. Pollaine, J. D. Salmonson, G. L. Strobel, L. J. Suter

February 17, 2005

Physics of Plasmas

Disclaimer

This document was prepared as an account of work sponsored by an agency of the United States Government. Neither the United States Government nor the University of California nor any of their employees, makes any warranty, express or implied, or assumes any legal liability or responsibility for the accuracy, completeness, or usefulness of any information, apparatus, product, or process disclosed, or represents that its use would not infringe privately owned rights. Reference herein to any specific commercial product, process, or service by trade name, trademark, manufacturer, or otherwise, does not necessarily constitute or imply its endorsement, recommendation, or favoring by the United States Government or the University of California. The views and opinions of authors expressed herein do not necessarily state or reflect those of the United States Government or the University of California, and shall not be used for advertising or product endorsement purposes.

Increasing robustness of indirect drive capsule designs against short wavelength hydrodynamic instabilities

S. W. Haan, M. C. Herrmann, T. R. Dittrich, A. J. Fetterman, M. M. Marinak, D. H. Munro, S. M. Pollaine, J. D. Salmonson, G. L. Strobel, and L. J. Suter

Lawrence Livermore National Laboratory
Livermore, CA 94550

Targets meant to achieve ignition on the National Ignition Facility [J. A. Paisner, J. D. Boyes, S. A. Kumpan, W. H. Lowdermilk, and M. S. Sorem, *Laser Focus World* 30, 75 (1994)] have been redesigned and their performance simulated. Simulations indicate dramatically reduced growth of short wavelength hydrodynamic instabilities, resulting from two changes in the designs. First, better optimization results from systematic mapping of the ignition target performance over the parameter space of ablator and fuel thickness combinations, using techniques developed by one of us (Herrmann). After the space is mapped with one-dimensional simulations, exploration of it with two-dimensional simulations quantifies the dependence of instability growth on target dimensions. Low modes and high modes grow differently for different designs, allowing a trade-off of the two regimes of growth. Significant improvement in high-mode stability can be achieved, relative to previous designs, with only insignificant increase in low-mode growth. This procedure produces capsule designs that, in simulations, tolerate several times the surface roughness that could be tolerated by capsules optimized by older more heuristic techniques. Another significant reduction in instability growth, by another factor of several, is achieved with ablators with radially varying dopant. In this type of capsule the mid-Z dopant, which is needed in the ablator to minimize x-ray preheat at the ablator-ice interface, is optimally positioned within the ablator. A fabrication scenario for graded dopants already exists, using sputter coating to fabricate the ablator shell. We describe the systematics of these advances in capsule design, discuss the basis behind their improved performance, and summarize how this is affecting our plans for NIF ignition.

This work was performed under the auspices of the U.S. Department of Energy by the University of California, Lawrence Livermore National Laboratory under contract No. W-7405-Eng-48.

I. INTRODUCTION

A number of target designs have been proposed to produce thermonuclear ignition on the National Ignition Facility (NIF) [1]. New targets are described here that are substantially less unstable hydrodynamically than previous designs. These targets, Fig. 1, use *indirect drive*: the laser heats the interior of a gold cylinder, a *hohlraum*, to very high temperature (250-300 eV) [2]. The x-rays filling the hohlraum ablate the outside of the spherical fuel capsule at its center, imploding and compressing deuterium-tritium (D-T) fuel. The fuel is initially in a spherical shell of solid D-T held at cryogenic temperature before the shot, self-smoothed by β -particle deposition from the T decay [3]. The laser pulse, Fig. 2, is tuned to launch four shocks and implode the capsule with the fuel close to Fermi-degenerate. This basic configuration has been the same since indirect drive ignition was first proposed for the NIF; the innovations described here pertain to the optimization of the ablator characteristics, both its dimensions and composition, and the layers of copper dopant in the ablator as they determine the hydrodynamic instability growth.

Several substances have been proposed for the ablator. Its material properties, primarily its opacity, control the hydrodynamic instability that can disrupt the implosion. (There is a substantial literature on these instabilities, reviewed in Ref. [2].) The instability growth determines specifications for roughness on the ablator and the D-T ice. Whether these specifications can plausibly be met determines the viability of a target; this and laser-plasma instabilities are the controlling features determining the size of the NIF facility.

The work described herein indicates that the use of radially graded copper dopant in beryllium confers remarkable stability on capsules for NIF, allowing them to tolerate surfaces 20 times rougher than typical first-generation NIF targets. With detailed optimization, uniformly doped Be(Cu) targets can also tolerate much rougher surfaces than the original designs—in this case about 8 times rougher. This substantial change in stability can allow for either significantly rougher surfaces than previously specified, or for reconfiguration of the target to accommodate other changes in the design. It probably relaxes the size requirement on tubes that could be used to fill capsules, making more feasible a fielding scenario in which the capsules are filled through a tube rather than being diffusion filled as originally proposed. This could allow for significant simplification of the cryogenic fielding hardware, since diffusion-filled capsules typically cannot hold the pressure at room temperature and must be kept cold once filled.

The first capsules considered for NIF assumed an ablator made of Be doped with ~1% Na and Br, radially varying within the shell. One such design, at 250 eV peak drive, is described in Ref. [2]. These early designs used a less optimal

grading scheme than described herein. The original Be(graded Na-Br) designs were supplanted in the planning and design by plastic capsules doped uniformly with Br, CH(Br) [4]. At that time it was believed that fabrication and fielding would be easiest with uniformly doped CH(Br). Targets were subsequently proposed with ablators of uniformly Cu doped Be [5], and of undoped polyimide [6]. Be is doped with Cu since it is known that Cu dissolves atomically in solid Be at the relevant concentrations of ~1%; the choice of dopant material is not tightly constrained by the implosion physics, provided that the dopant increases the opacity to hard x-rays while minimally increasing the opacity for the bulk of the x-rays in the drive. CH capsules can be doped with either Br or Ge. Polyimide, with its O and N content, is best left undoped at 300 eV, and is too opaque to make a good ablator at 250 eV. These three ablators—polyimide, CH(Ge), and Be(Cu), all uniformly doped or undoped—have been the mainline NIF targets, and considerable work has been done investigating their features [7,8,9]. Concurrently, some work was done with radially graded dopants. Dittrich [10] described a 250 eV Be(graded Cu) design, implementing a scheme attributed to Hatchett (unpublished) and considered in more detail below. Another graded dopant approach, with a layer of clean Be inside of an otherwise uniformly doped Be(Cu) shell, was considered in a 350 eV Be(Cu) design by Hinkel [11].

All the early targets were heuristically optimized: the designers used guidelines based on two dimensional simulations and physical principles to optimize a design in one dimension, and its properties were explored in two and three dimensions (2D and 3D). The scans used for optimization were expanded to scans over one parameter, [10] and then the two parameters of ablator and fuel thickness [12]. As described in more detail below, the optimization process has now been automated by one of us (Herrmann) allowing for much more detailed scans over the parameter spaces of possible designs. Given these detailed scans, more systematic 2D optimization is also possible. That process is described below and then used to consider the impact of varying dopant concentration, for uniformly doped Be(Cu) targets.

Once the uniformly doped targets have been fully optimized, the next possibility to consider is spatially varying the dopant. One such design from Ref. [10] was meant to explore the limits of extremely small size and low temperature, to see whether such a design might feasibly work. Hence it very small, and driven at low temperature (250 eV). That work concluded that the capsule was too marginal to be feasible as a proposed design. Larger scales of Dittrich's design were not considered at that time. Subsequently, Strobel *et al.* [12,13] and Bradley *et al.* [14] examined uniformly doped 250 eV Be(Cu) designs using more typical NIF power and energy. They found that, in order to be comparable to the Dittrich design in margin against hydrodynamic instability growth, the uniformly doped targets required considerably more power and energy than the Dittrich design. This suggested that the Hatchett-Dittrich doping scheme conferred more

stability than originally recognized. Haan's original 250 eV design [2], with graded dopant but less well optimized, was intermediate in stability (the three designs are compared in Ref.13). In the following, the Dittrich design is examined at scales comparable to those considered in refs. [12-14], and is found to be substantially more stable. The same graded-dopant scheme is also implemented in a 300 eV design, at a baseline power-energy scale, and it is also much more stable than any other design at comparable power and energy.

Many of the fabrication considerations that led to preference of CH over Be(Cu) have changed so that Be is now considered very attractive for fabrication. One consideration, the possible roughness of the surface, is addressed directly by the design concepts described here, since these designs can tolerate significantly rougher surfaces. Characterization of the ice layer inside of the optically opaque Be has been demonstrated using x-ray refractive imaging [15,16]. CH had been considered advantageous because it leaves open the possibility of smoothing the layer with infrared deposition, but the layers seen inside of Be with only β energy deposition appear to be adequate, especially given the reduced stability requirement with graded dopant. Finally, diffusion fill had been thought to be advantageous since it eliminated a fill tube, and it was thought that Be could not be diffusion filled. However, the fielding simplifications resulting from the use of a fill tube are now thought to be more important than the deleterious impact of the tube. Fabricating the layers of varying Cu concentration is a straightforward extension of technology already being developed for Be ablaters, using sputtering coating: the Cu concentration can be varied in time as the coating is deposited.

The remainder of this paper is as follows. Section II has details of the simulation techniques. Sections III, IV, and V describe the Be(Cu) designs we are considering here; Section VI compares these targets via 2D simulations. Section VII is a conclusion.

II. SIMULATION DETAILS

The simulations described here were done with the codes Lasnex [17] and Hydra [18]. One-dimensional simulations were done with full multi-group radiation transport, and with multi-group radiation diffusion. The diffusion simulations use a mean-free-path-to-boundary scheme and few-group weighted opacities, and have the drive spectrum adjusted slightly to make them more closely match the 1D simulations with full transport. They reproduce highly resolved 1D multi-group transport simulations to about 1% in all of ablation rate, implosion history, and density profiles. Two-dimensional simulations used to evaluate the hydrodynamic instability growth use the same diffusion setup. They have been done with XSN opacities [19], and with opacity tables generated [20] using the Opal [21] model for the low atomic number ions and the super-transition-array (STA) [22] model for the Cu. The two opacity models give essentially

identical results. Most of the simulations have been done with QEOS equation of state [23], with parameters set so that the D-T EOS is intermediate within the range seen in recent experiments [24-26]. The simulations use a frequency-dependent source, with a spectrum extracted from gold hohlraum simulations. The M-band content in the spectrum is similar to that described in Ref. 12.

There are two ways to simulate the growth and impact of hydrodynamic instability growth. Single modes can be initialized with small amplitudes so that they stay linear throughout the implosion. Such simulations are used to evaluate the amount of instability growth for each individual modal perturbation. To simulate the net impact of the instability growth it is necessary to do simulations that include a wide spectrum of modes, with realistic initial amplitudes. Multi-mode simulations have been done for the capsules described here, using the spectrum of initial perturbations described in Ref. [10]. When the rms is 10 nm, this spectrum corresponds to the high-mode part of the “NIF standard” spectrum used by the target fabrication community as a roughness goal [27]. Various surface roughnesses are modeled by multiplying the perturbation by an overall multiplier. Only modes 12 and above are typically included in these simulations (lower modes can be included in other simulations as described below). The power in each 2D mode is multiplied by $(2l+1)$ in order to represent the 3D power spectrum as well as possible.

III. OPTIMIZATION OF UNIFORMLY DOPED Be(Cu) DESIGN

A new way to optimize of capsules has been developed by one of us (Mark Herrmann). Herrmann's innovations have been a better implementation of the constraints than previously, and an automated process that thoroughly optimizes over the remaining free parameters. Ultimately the true constraints are on hohlraum size, as that determines the energy and power needed to heat the hohlraum, and on the temperature vs. time profile as determined by the laser power and energy. These in turn constrain (i) the capsule size, as that affects hohlraum-to-capsule size ratio, (ii) the peak temperature T_R , and (iii) to a good approximation, the time integral of $T_R^4(t)$. This set of constraints is slightly different from past work[12], where we regarded the absorbed energy as the primary quantity to hold fixed. Herrmann argues that capsules with lower albedos, which can absorb more energy at given size and T_R , should not be "punished" for this better performance. Thus the capsule absorbed energy is not constrained in the optimization, although of course it does not vary very much for a given material, given the constraints on outer radius, peak T_R , and integral of $T_R^4(t)$.

After we fix these three parameters, a capsule design is characterized by ablator material, ablator thickness, fuel thickness, and the detailed shape of $T_R(t)$. For a given ablator material, and assuming that we can optimize $T_R(t)$, that leaves a two-dimensional parameter space of fuel thickness and ablator thickness. At each point in this space,

Herrmann's scheme automatically adjusts the drive profile using a set of scripts running LASNEX or HYDRA and adjusting the profile to produce optimal shock timing as described by Munro [28]. A scan over the thicknesses then provides a map of yield in the two dimensional parameter space of shell thicknesses, as shown by the yield contours in Fig. 3. When the ablator is too thin, it burns through and the target fails to ignite. When the shells are too thick, the velocity is inadequate and again the target fails. In between is the operating space.

This procedure is the maturation of an approach described by Dittrich [6,10], who did scans over ablator thickness at constant fuel mass, and by Strobel [12] who did a 2D scan over ablator and fuel thickness similar to what Herrmann has done. Dittrich and Strobel both tuned the individual designs by hand, so the scans were necessarily less complete and more noisy, and they kept absorbed energy fixed rather than outer radius. All of the results have given very similar results; the modern technique allows for more accurate and complete scans, and more of them.

Having defined the space of one-dimensional performance, we can then explore the 2D (and presumably 3D) characteristics. As shown in Fig. 3, short-wavelength Rayleigh-Taylor is generally worse as we move towards thinner shells within this space. Sensitivities to longer wavelength capsule defects, or to asymmetry, depend more on deceleration Rayleigh-Taylor and accordingly are worse for the lower velocity targets with thicker shells. Because the short-wavelength Rayleigh-Taylor has more e-foldings of growth, it is generally more sensitive, i.e. the overall optimization tends to be more influenced by the short wavelengths than the long, pushing us towards thicker shells than previously thought optimal. Once the implosion velocity is above about $37 \text{ cm}/\mu\text{s}$ (at 1.11 mm outer radius for plastic capsules) the long wavelength robustness does not increase very much with velocity, so the optimum design is probably that which has velocity just at $37 \text{ cm}/\mu\text{s}$. While this specific optimization is valuable, the most important product of this work is a quantification of the tradeoff, and the creation of the tools to evaluate the whole space of targets. Future work will change the specifics, and tell us which source of perturbation is dominant; now we have the tools to evaluate the relative importance of future results.

This scan technique has been applied to a variety of targets, including: the CH(Ge) "scale 1" 300 eV capsule shown in Fig. 3; polyimide at the same outer radius and peak drive; Be(Cu) under the same conditions, as described in more detail below; and three ablator materials at 250 eV: CH(undoped), polyimide, and Be(Cu). We find that at 250eV, undoped CH has similar yield to uniformly doped Be(Cu), and can tolerate similar surface roughness (about 75 nm in spherical harmonic modes above 10, assuming a standard surface power spectrum, at a scale where the capsule absorbs

350 kJ). At this low drive temperature, both are considerably superior to polyimide, which gives similar yield but requires the ablator surface to be a factor of several smoother.

We have done this optimization for Be(Cu) designs at various Cu concentrations. At lower Cu levels the targets optimize with relatively thicker ablaters, as expected. All targets had 1110 μm outer radius, 0.3 mg/cc D-T gas density, and a source corresponding to 1.4 MJ of laser energy absorbed by a standard gold hohlraum. Scans for the two extreme Cu levels are shown in Fig. 4. We then selected a similarly optimized design at each of several Cu concentrations: 0.4%, with dimensions 175x80; 0.7%, 158x80; 0.9%, 150x80; 1.1%, 145x80; and 1.5%, 133x80. In addition to having the same fuel thickness, these all have the same implosion velocity of $3.7e7$ cm/s. Yields are all very close to 20 MJ. More details about these designs will be presented below, in comparison with the graded doped designs.

IV. 5 layer graded doped designs

When Strobel *et al.* [12] did an optimization of 250eV Be(Cu) capsules, similar to that described above although less complete, they found that their optimized 250eV target at 190 kJ was not much more robust than a 5-layer graded doped design published by Dittrich [10] that only absorbed 95 kJ. That suggested that graded doped capsules were superior to uniformly doped capsules, although they had never been compared in detail. (Strobel's optimization, while crude, has been confirmed by application of the technique described above.) The design in Ref. 10 was very small, intended to probe the limits of what capsules may ignite on NIF. Dittrich did not consider larger scales. We have now found that when the target is taken to larger scales it is remarkably less sensitive to ablator roughness than are the uniformly doped Be(Cu) capsules. This comparison is shown in Fig. 5. Dittrich's design was optimized with 1D simulations, scanning over a few 1-dimensional parameter variations, as described in Ref. 10. It seems plausible that it could be better optimized using variations on the techniques described above, but such an optimization has not yet been attempted. The larger targets are simple geometrical scales of Dittrich's. They were not reoptimized in any way except minor heuristic changes in an overall multiplier on the dopant level, and pulse shape adjustments.

A design at 300 eV was based on Dittrich's design: the thicknesses are essentially the same as an appropriate scale of the 250 eV design, but the radius was decreased and the dopant level increased. This results in a 300 eV design, shown in Fig. 1, the performance of which is described in more detail below. This target has also not yet been systematically optimized; it is based on a few heuristic changes from the 250eV design. Remarkably it is nevertheless considerably more robust than any other target at this scale.

V. 2 layer graded dopant design

The two desirable features of a graded doped design are (i) a low dopant on the outside, to minimize instability growth during acceleration; and (ii) an undoped region immediately next to the fuel, which will preheat less, hence staying at higher density and reducing instability growth at the fuel/ablator interface. The simplest way to achieve this is to take a low-level doped design and replace some of the inner ablator with undoped Be. (Hinkel *et al.* [11] used a similar two-layer scheme for a 350 eV target design.) As described below, we found that the 0.4% uniformly doped design had very desirable ablative instability features but too much short-wavelength growth at the interface; that suggested that it could be the basis for a two-layer design, simply by replacing an inner layer of the 0.4% doped Be with clean Be. The appropriate amount of clean Be can be found by varying the thickness of the clean layer, as shown in Fig. 6. If the undoped layer is too thick, it begins to ablate and the material next to the fuel is no longer protected from preheat. The density next to the fuel is maximized for a clean thickness of about 5 μm . This defines our 2-layer design: the same as the 0.4% design optimized above, but with the inner 5 μm of Be undoped.

Neither graded doped capsule has yet been systematically optimized; doing so may or may not improve performance beyond the heuristically optimized current designs. Dittrich's original small scale 250 eV graded doped design was optimized with a moderately systematic approach, not quite as elaborate as modern techniques allow.

Note that the uniformly doped targets, and the 2-layer graded dopant, have outer radius 1110 μm while the 5-layer design is 1105 μm . This small inadvertent inequivalence, a historical artifact, could be responsible for a few-percent increase in the specifications for the larger targets (in which case a truly equivalent comparison would increase even further the superior performance of the 5-layer design).

VI. Comparison of designs via 2D simulations

The in-flight density profiles for the 5 capsules considered here are shown in Fig. 7. The uniformly doped capsules show the expected dependence on dopant: more highly doped capsules have a steep, unstable ablation front, while the most lightly doped capsules are more stable at the ablation front but have a large density step at the outside of the fuel. The 2-layer design has the desired high density region just outside the fuel, while the 5 layer design has both the high density region and the best ablation front features.

The most direct way to compare the stability of the designs is with multi-mode 2D simulations that vary the initial amplitude. Initial perturbations were in modes 12-160, with the spectrum as in Ref. 10. The result of doing so is shown in Fig. 8 for the three uniformly doped targets. By this way of evaluating the growth, the 0.4% target is the most robust. However, this target has substantial short wavelength growth as described below.

A similar plot showing the graded doped designs is in Fig. 9. They are much more stable. The 5-layer design is somewhat more stable than the 2-layer design, although the latter is quite a bit better than any of the uniformly doped designs from Fig. 8. Fig. 9 shows a few variants on the 5-layer design, indicating the sensitivity to central gas density and composition, and to the specifics of the dopant profile.

The stability of these targets does not appear to be a result of fine optimization of the dopant profile. As evidence for that, Figs. 9 shows 2D simulations of a design in which the inner two steps of the dopant profile from the 5-layer design are replaced with a constant dopant concentration at the highest level of 0.7%. This increases the instability growth only slightly. From a functional optimization point of view, it appears that the optimum is fairly broad; if the dopant is not constrained to be uniform, there is a wide variety of profiles that give performance better than any uniform dopant level.

The other way to examine the growth of perturbations is to do simulations of one mode at a time. These are easier to validate, and can be easier to understand. Growth factor calculations are shown in Fig. 10. The low hot-spot growth is only at low modes and is consistent with the trends evident in the multi-mode simulations as shown in Figs. 8 and 9. The growth to the fuel/ablator interface at peak velocity, Fig. 10b, is much more complex. The only target that clearly shows ablative stabilization of the high modes is the 1.5% uniformly doped design, which has the worst intermediate-mode performance. The graded-doped designs show intermediate growth of high modes. One reason why the 5-layer design is so robust in multi-mode simulations is that it has low growth around mode 150, the highest modes included in these simulations. It is the growth of these modes that is responsible for the worse performance of the 2-layer design in the multi-mode simulations. This may be an artifact of the cutoff in the simulations and needs to be investigated further.

Another very important high-mode issue is the perturbations seeded at internal interfaces. In this case the 2-layer design is clearly inferior to the 5-layer design. Growth of perturbations seeded at the fuel/ablator interface as simulated to date show less growth than those seeded at the internal interfaces, although they have not yet been studied exhaustively. Clearly there is considerable work that needs to be done exploring the high mode growth seeded by the various interfaces, as well as the beryllium microstructure.

In the actual experiment these high modes may or may not matter, depending on the spectrum of initial perturbations, as they determine whether the shell survives past peak velocity. The high modes might be more important to the growth of perturbations seeded by a fill tube, which is initially at very high mode number. Fill tube simulations are in progress for both the uniform and the graded doped capsules as described in another article in this issue [29].

Very low modes (about 10 and below) have been simulated for these targets and do not vary significantly from target to target. That is consistent with the fact that all the targets have essentially the same fuel mass and implosion velocity.

Ice roughness perturbations have been studied only very slightly at the time of this writing, except to check that the nominal 5-layer graded doped capsule can tolerate ice roughness of about 5 microns rms with a standard spectrum. This is substantially more than previous capsules, which could typically tolerate 1-2 μm . A quantitative comparison of the new targets remains to be done.

This work has increased our awareness of very short wavelength growth, and it is clear that more analysis is needed of the high modes seeded at the various interfaces and by the beryllium microstructure. Also, work is needed on how the surface perturbations combine with other sources of perturbation. A preliminary pass on this has been done: multi-mode simulations were done with nominal perturbations on all of the interfaces, in modes 2-160. They perform close to 1D. A detailed rollup of the relative impact of all of the sources of uncertainty, for the new targets, is being developed for future publication.

VII. Conclusion

Redesign of the NIF targets has resulted in targets that can tolerate substantially larger perturbations than the original designs, as shown in Fig. 9. Systematic optimization of uniformly doped capsules increased the tolerable surface roughness for CH(Ge) capsules to 65 nm, about twice what it was previously, and for uniformly doped Be(Cu) targets to more than 200 nm. (The actual specifications for surface roughness must leave margin for other sources of error, and these numbers are the ablator roughness at which roughness alone degrades the yield. Hence the specification is about 1/3 of the numbers given here.) Three designs have been examined using graded Cu dopant in the Be, and they can tolerate a roughness of up to 600 nm, about 20 times larger than typical previous targets. This reduced instability growth should provide margin for optimization of whatever source of imperfection in the implosion is ultimately the most important.

References

- [1] J. A. Paisner, J. D. Boyes, S. A. Kumpan, W. H. Lowdermilk, and M. S. Sorem, *Laser Focus World* 30, 75 (1994)
- [2] J. D. Lindl, *Inertial Confinement Fusion* (Springer-Verlag, New York, 1998).
- [3] A. J. Martin, R. J. Simms, and R. B. Jacobs, *J. Vac. Sci. Technol. A* 6 (3), 1885 (1988).
- [4] S. W. Haan, S. M. Pollaine, J. D. Lindl *et al.*, *Physics of Plasmas* 2, 2480 (1995).
- [5] D. C. Wilson, P. A. Bradley, N.M. Hoffman *et al.*, *Physics of Plasmas* 5, 1953 (1998)
- [6] T. R. Dittrich, S. W. Haan, S. M. Pollaine, and A. K. Burnham, *Fusion Technology* 31, 402 (1997).
- [7] M. M. Marinak, S. W. Haan, T. R. Dittrich, R. E. Tipton, and G. B. Zimmerman, *Phys. Plasmas* 5, 1125 (1998).
- [8] W. J. Krauser, N. M. Hoffman, D. C. Wilson *et al.* *Phys. Plasmas* 5, 1125 (1997).
- [9] M. M. Marinak, G. D Kerbel, N. A. Gentile *et al.*, *Phys. Plasmas* 8, 2275 (2001); T. R. Dittrich, S. W. Haan, M. M. Marinak *et al.*, *Phys. Plasmas* 6, 2164 (1999).
- [10] T. R. Dittrich, S. W. Haan, M. M. Marinak *et al.* *Phys. Plasmas* 5, 3708 (1998).
- [11] D. E. Hinkel, S. W. Haan, A. B. Langdon *et al.* *Phys. Plasmas* 11, 1128 (2004).
- [12] G. L. Strobel, S. W. Haan, D. H. Munro, and T. R. Dittrich, *Phys. Plasmas* 11, 4261 (2004)
- [13] G. L. Strobel, S. W. Haan, D. H. Munro *et al.*, *Phys. Plasmas* 11, 4695 (2004).
- [14] P. A. Bradley and D. C. Wilson, *Phys. Plasmas* 6, 4293 (1999).
- [15] D. S. Montgomery, A. Nobile, and P. J. Walsh, *Rev. Sci. Instrum.* 75, 3986 (2004).
- [16] B. J. Kozioziemski, J. A. Koch, A. Barty, *et al.*, to be published in *J. Applied Phys*, March 1 (2005).
- [17] G. B. Zimmerman and W. L. Kruer, *Comments Plasma Phys. Controlled Fusion* 2, 51 (1975).
- [18] M. M. Marinak, R. E. Tipton, O. L. Landen *et al.*, *Phys. Plasmas* 3, 2070 (1996).
- [19] See National Technical Information Service Document No. UCRL-52276 [W. A. Lokke and W. H. Grasberger, in *Lawrence Livermore National Laboratory, UCRL-52276, (1977)*]. Copies may be ordered from the National Technical Information Service, Springfield, Virginia 22161. The price is \$19.50 (\$4.00 for microfiche) plus a \$3.00 handling fee. All orders must be prepaid. G. B. Zimmerman and R. M. More, *J. Quant. Spectrosc. Radiat. Transfer* 23, 517 (1980); R. M. More, *ibid.* 27, 345 (1982).
- [20] John Castor (private communication)
- [21] F. J. Rogers and C. A. Iglesias, *Science* 263, 50 (1994); C. A. Iglesias and F. J. Rogers, *Astrophys. J.* 464, 943 (1996)

- [22] Bar-Shalom A. and Oreg J., Phys. Rev. E, 54, 1850 (1996).
- [23] R. M. More, K. H. Warren, D. A. Young, and G. B. Zimmerman, Phys. Fluids 31, 3059 (1988).
- [24] L. B. Da Silva, P. Celliers, G. W. Collins et al., Phys. Rev. Lett. 78, 483 (1997); G. W. Collins, P. Celliers, L. B. Da Silva, *et al.*, Phys. Plasmas 5, 1864 (1998).
- [25] M. D. Knudson, D. L. Hanson, J. E. Bailey, C. A. Hall, and J. R. Asay, Phys. Rev. Lett. 87, 225501 (2001).
- [26] T. R. Boehly, D. G. Hicks, and P. M. Celliers, Phys. Plasmas 11, L49 (2004).
- [27] R. C. Cook, R. McEachern, and R. B. Stephens, Fusion Technol. 35, 224 (1999).
- [28] D. H. Munro, P. M. Celliers, G. W. Collins, *et al.*, Phys. Plasmas 8, 2245 (2001).
- [29] M. J. Edwards *et al.*, Phys. Plasmas this issue.

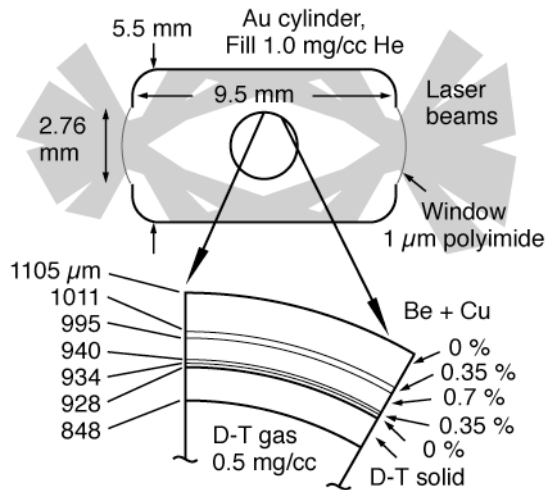


Fig. 1. Target proposed to achieve ignition on the National Ignition Facility. Inset shows a capsule with 5-layer graded doped beryllium ablator, using the indicated copper concentrations.

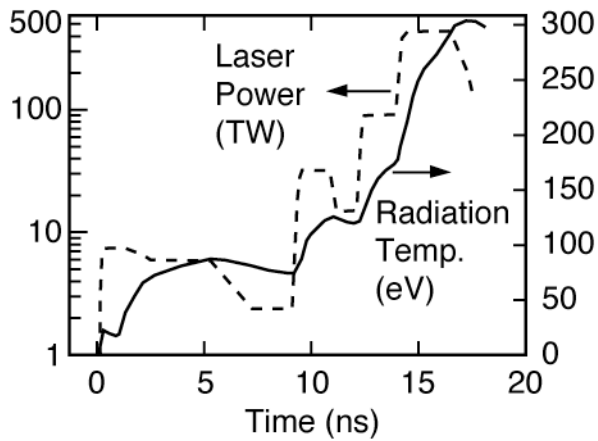


Fig. 2. Laser power to drive the target, and the corresponding temperature vs. time in the hohlraum. This baseline target uses 1.4 MJ of 0.3 μm light absorbed in the target, at peak power 410 TW. The capsule absorbs 180 kJ, and produces 19 MJ of fusion energy.

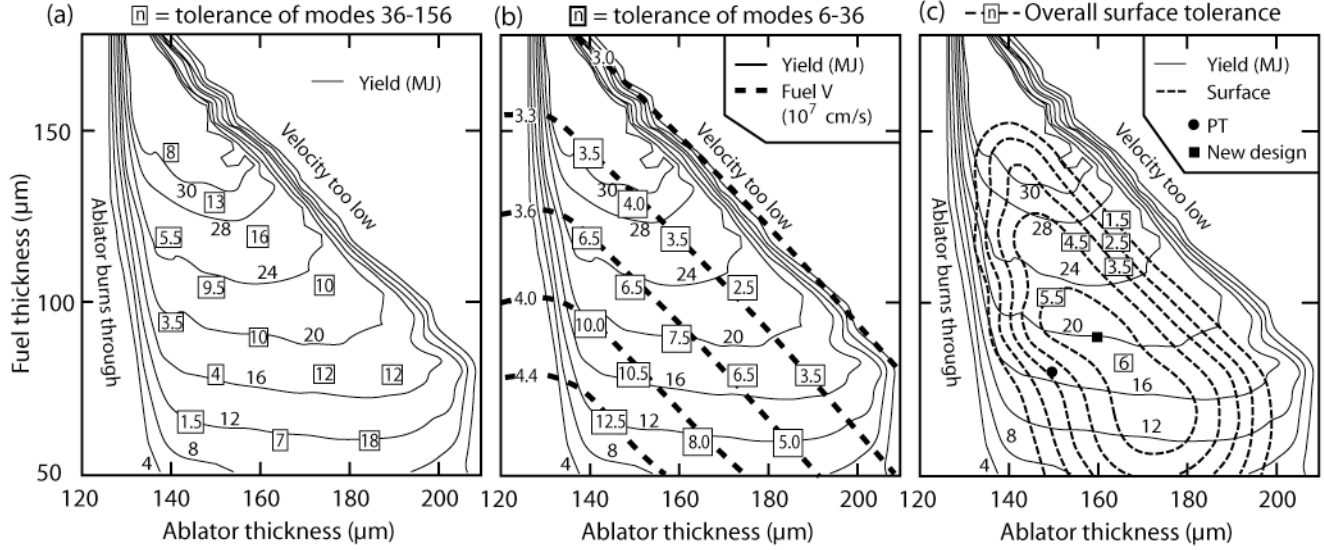


Fig. 3. Performance of uniformly doped CH(Ge) capsules vs. thickness of ablator and fuel. At each set of dimensions the pulse-shape driving the capsule is optimized by an automated routine. Ge concentration is fixed at 0.25%. The outer radius is held fixed at 1.110 mm, the peak T_R at 300 eV, and the integral of $T_R^4(t)$ is held fixed at a scale corresponding to 1.4 MJ of absorbed laser energy. Contours show the yield as a function of capsule dimensions, with overlays as follows. (a) The numbers in squares indicate the ablator roughness in modes 36-156 that degrades the yield in 2D simulations by 50% relative to no roughness. In (b) the numbers indicate the roughness in modes 6-36 that causes 50% yield reduction. Contours of peak implosion velocity are also indicated, showing that the sensitivity to these low modes is a function primarily of implosion velocity. In (c) the net roughness requirement for all modes is shown. It assumes that the roughnesses as describe in (a) and (b) combine in quadrature; the validity of using the quadrature sum was checked for the central point that could tolerate the roughest surface.

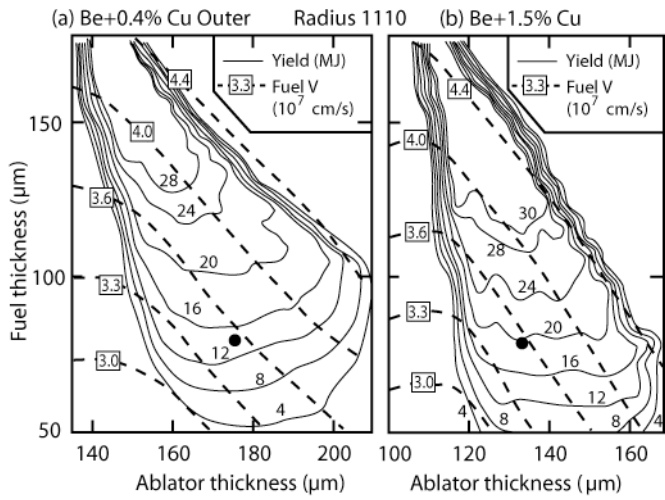


Fig. 4. Scans over ablator and fuel thickness for two extremes in Cu concentration: (a) 0.4% and (b) 1.5%. Similar scans were done for 0.7%, 0.9%, and 1.1%, with features intermediate between those shown here. The points indicated with black dots are designs selected for 2D comparison.

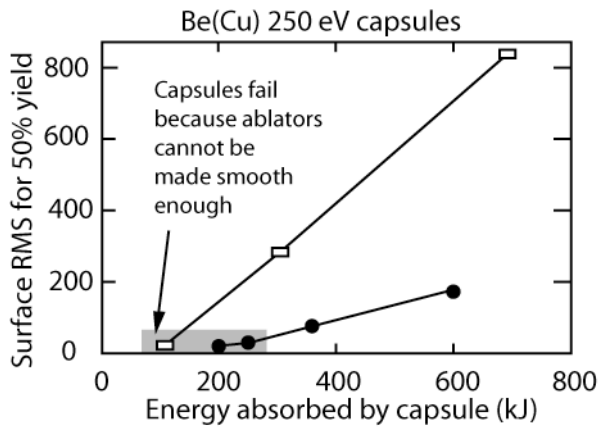


Fig. 5. For 250 eV Be(Cu) designs, the ablator roughness requirement vs. capsule absorbed energy. The upper curve shows new simulations of scales of the Dittrich graded dopant design[10], similar to that shown in Fig. 1, with the left-most point being Dittrich's design. The lower curve is for an optimized uniformly doped design (curve taken from Ref. 13).

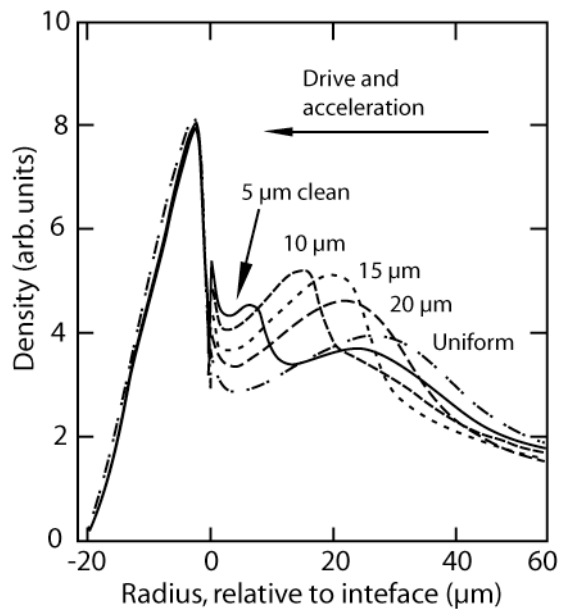


Fig. 6. Density vs. radius, in flight at a radius somewhat below half initial, for a series of designs with varying thickness of clean beryllium inside of 0.4% Be(Cu). All targets are 175 μm total Be thickness, and had the same drive.

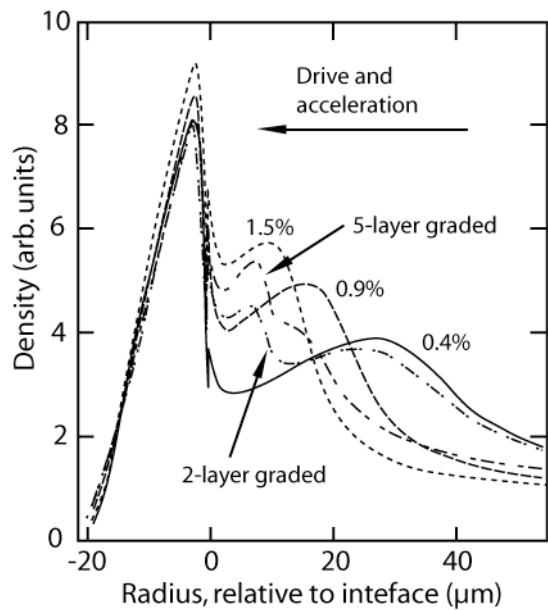


Fig. 7. Density vs. radius, in-flight at a radius somewhat below half initial, for the graded and uniformly doped Be(Cu) capsules.

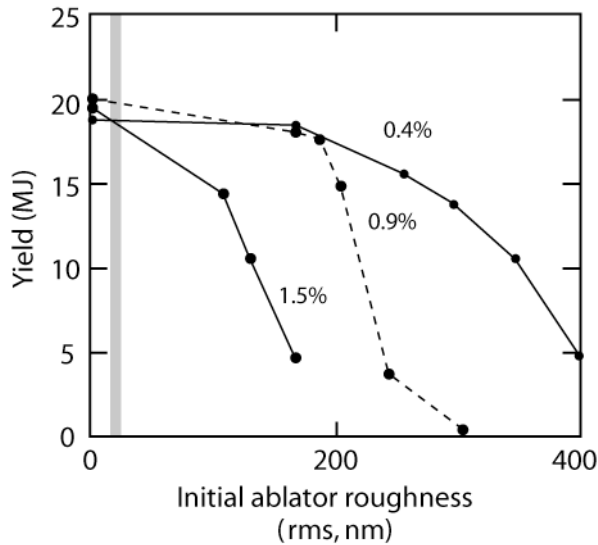


Fig. 8. Yield vs. initial ablator roughness for the three uniformly doped designs. These simulations include modes 12-160, and assume the same power spectrum for the perturbations, described in the text. The gray bar shows the roughness of existing plastic capsules, at the “NIF standard” surface roughness.

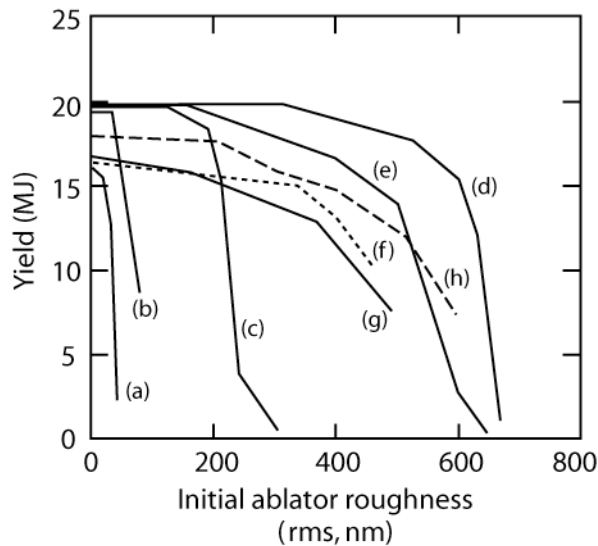


Fig. 9. Yield vs. roughness for graded doped capsule designs compared to previous designs. The capsules are all “scale 1,” requiring about 1.4 MJ of laser energy absorbed in a 300 eV hohlraum. Solid curves are different designs, at central gas 0.3 mg/cm^3 , and dashed curves show variants on curve d, the design from Fig. 1. (a) plastic capsule prior to 2003; (b) recent reoptimization, CH(Ge); (c) recent reoptimization, uniformly 0.9% doped beryllium; (d) graded doped beryllium, design shown in Fig. 1; (e) the 2-layer design described in the text; (f) same as d, except central gas D-T density 0.5 mg/cm^3 ; (g) same as f, with $8 \mu\text{g/cm}^3$ of ^3He also included; (h) same as d, but inner two steps of grading replaced with uniform 0.7% Cu.

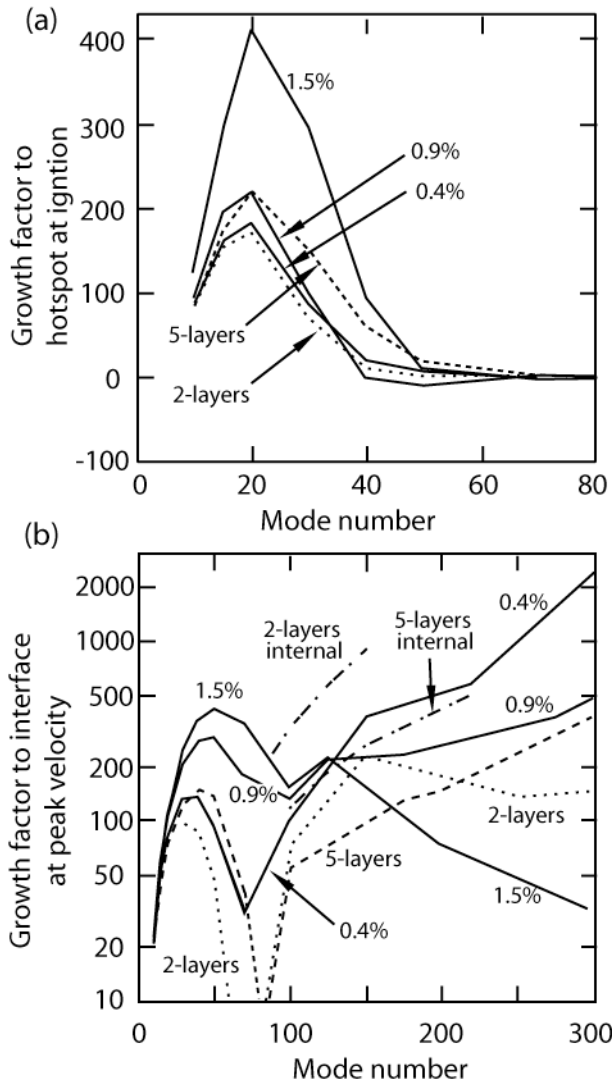


Fig. 10. Growth factors vs mode number from linear-regime 2D simulations. Solid curves are graded doped capsules, dashed uniformly doped. (a) Perturbation initially on Be outer surface, to perimeter of hot spot at ignition, i.e. 1% burn rate contour when central temperature is 12 keV. (b) Be outer surface, to fuel/Be interface at peak velocity. These curves are envelopes of maximum growth, and do not show intermediate modes with less growth. The full growth-factor curves have considerable structure vs. mode number. Dot-dash curves labeled “internal” are for perturbations initially on internal interfaces between the dopant layers. For the 2-layer design there is only one such interface, with growth factors indicated. For the 5-layer design the three inner interfaces have growth factors close to the indicated curve, while the more external interfaces have much smaller growth factors.